Journal of Material Science and Mechanical Engineering (JMSME)
p-ISSN: 2393-9095; e-ISSN: 2393-9109; Volume 3, Issue 6; July-September, 2016 pp. 427-432

http://www.krishisanskriti.org/Publication.html

Study into the Performance of Activated TIG Process in AISI 316 Stainless Steel Weldments

Kashish Kumar[1] and Shankar Singh[2]

[1,2]Department of Mechanical Engineering, Deemed University,)Sant Longowal Institute of Engineering and Technology, Sangrur, Punjab-148106, India
E-mail: [1]kash10oct10@gmail.com, [2]singh.shankar@gmail.com

Abstract—*Tungsten inert gas (TIG) welding continues to be one of the major welding processes used in the industry for high quality weld joints. The published work reports that the major limitations of TIG welding of steels are due to the limited thickness of material which can be welded in a single pass, poor tolerance, cast variations and the low productivity. An increase productivity can be achieved by increasing the penetration depth, as it helps reducing the number of welding passes. Activated TIG (A-TIG) welding process can be beneficial in this respect. .In the present study an attempt has been made to understand the effect of A-TIG welding parameters such as type of welding, welding current, gas flow rate, welding speed that influences performance measures such as tensile and impact strength of weld joint by using Taguchi optimization technique. The effort to predict optimal parametric settings and their contribution on producing better weld quality and higher productivity has been discussed. The experimental results indicated that the increase in the tensile and impact strength is significant with the use of TiO_2 flux.*

Keywords*: TIG,A-TIG, Activated flux, 316 Stainless steel, Taguchi's Methodology, optimization.*

1. INTRODUCTION

Welding, a fabrication process is used to join materials that can be either metals or thermoplastics. The TIG welding is considered to be a pivotal arc welding processes. The TIG welding process provides high quality metallurgical weld having good mechanical properties [1]. One of the limitation of the TIG welding process is low penetration depth. Literature identifies that these limitations can be recovered up to some extent by using activated flux. Although tungsten inert gas (TIG) welding can produce a high-quality weld, its application is usually limited to thin plates welded by a single-pass procedure, and the process also suffers from relatively low productivity. The low productivity of TIG welding results from a combination of a low deposition rate and shallow joint penetration. The TIG welding with activated flux is a notable arc welding that can dramatically increase the joint penetration [2].This variant of TIG welding and is called activated TIG (A-TIG) welding. A-TIG welding intensifies the conventional TIG (C-TIG) welding process, allowing for the joining of thick plate single-pass operation without edge preparation and filler metal, instead of using multi-pass welding procedures. The present work focuses on the study of effects of surface active fluxes on tensile and impact strength on weld specimen by using TIG [3-11].

2. LITERTURE REVIEW

Karunakaran et al.(2012) performed TIG welding of AISI 304L stainless steel and compare the weld bead profiles for constant current and pulsed current setting[12]. Effect of welding current on tensile strength, hardness profiles, microstructure and residual stress distribution of welding zone of steel samples were reported.

Vasudevan et al.(2015) studied the A-TIG process on DMR249 Steel[13].Design of experiments (DOE) approach was employed using response surface methodology for achieving maximum(RSM) and Taguchi technique to optimize the welding parameters for achieving maximum depth of penetration in a single pass. Design matrix was generated using DOE techniques and bead on plate experiments were carried out to generate data for influence of welding process variables on depth of penetration.

3. EXPERIMENTATION

The Stainless steel AISI 316 is one of the most commonly used material in manufacturing industries because it has better corrosion resistance and good weldability. The stainless steel 316 is used to conduct the test. The mechanical properties and composition of Stainless Steel 316 are shown in the Tables 1 and 2, respectively [10].

Table 1 Mechanical Properties of 316 Stainless Steel

Tensile stress(MPa)	Yield stress(MPa)	Poission ratio	% Elongation
580	290	0.265	40 min

Table 2 Composition of SS 316

Elements	C	Mn	P	S	Cr	Mo	Ni	Si
%	0.08	2	0.045	0.03	16-18	2-3	10-14	0.75

The properties of TiO_2 flux used as activated flux is shown in Table 3[11].

Table 3: Properties of TiO_2 Activated Flux

Property	Values
Molar mass (g/mol)	79.866
Appearance	White solid
Density (g/cm3)	4.23
Solubility in Water	Insoluble

3.2 Taguchi Method and Design of Experiment

Taguchi method is a powerful problem solving tool, which can improve the performance of the product quality, process, design and system with a great decrease in experiment time cost.[14] This method which contains the design of experiment theory and quality loss function concept has been carrying out robust design of processes and products and solving several optimal problems in manufacture industries. Taguchi develops a methodology for finding the optimum settings of control factors and making a product or process insensitive to noise factors [15].To resolve the complexity Taguchi's methodology works as follows; first, the experiments are planned according to the optimized problems with noise factors & control factors being identified. Noise factors are those which cannot be changed during experimentation, whereas the control factors can be changed during experimentation. Orthogonal array test on the basic factors is then selected, and the experiments are carried out on the basis of designed orthogonal array. The best levels for the factors are then confirmed after some complicated data analysis using some S/N ratio. There are three kinds of quality characteristics in the analysis of S/N (signal to noise) ratio, such as the larger the better, the smaller the better and the nominal the better. The S/N ratio is calculated based on the S/N analysis function. Generally a larger S/N ratio is consistent with better quality characteristics. Moreover, the ANOVA is to investigate which process parameters significantly affects the quality characteristic with the S/N ratio results.

Smaller the better:

$$\frac{S}{N} = -10\log(\frac{1}{n}\sum_{i=0}^{n} y_i^2) \quad (1)$$

Larger the better:

$$\frac{S}{N} = -10\log(\frac{1}{n}\sum_{i=0}^{n} \frac{1}{y_i^2}) \quad (2)$$

Factors A is type of welding where as factor B,C,D are current(A), shielded gas flow rate(l/min) and welding speed(mm/min) respectively.

3.3 Parameter and Performance Measures

In this study, four main parameters of TIG process including type of welding with two levels and welding current, gas flow rate and welding speed were evaluated at three levels. Taguchi experimental layouts are shown in Table 4.

Table 4: Process Parameters and their Levels

Name of factor	Symbol (Unit)	Level		
		1	2	3
Type of Welding	-	C-TIG	A-TIG	-
Current	I(A)	110	130	150
Shielded Gas Flow Rate	SGFR(l/min)	8	10	12
Welding Speed	V_w (mm/min)	70	85	100

3.4 PROCEDURE

For this purpose, plates with the dimensions of 70×50×6 mm were prepared and tests were conducted. The experimental runs were planned on the basic of L18 ($2^1 \times 3^3$) orthogonal array with 18 test runs.

Table 5: Taguchi L_{18} Orthogonal Design

Runs	Noise factors	Control factors		
	Type of Welding	Current(A)	SGFR (l/min)	Welding Speed (mm/min)
1	C-TIG	110	8	70
2	C-TIG	110	10	85
3	C-TIG	110	12	100
4	C-TIG	130	8	70
5	C-TIG	130	10	85
6	C-TIG	130	12	100
7	C-TIG	150	8	85
8	C-TIG	150	10	100
9	C-TIG	150	12	70
10	A-TIG	110	8	100
11	A-TIG	110	10	70
12	A-TIG	110	12	85
13	A-TIG	130	8	85
14	A-TIG	130	10	100
15	A-TIG	130	12	70
16	A-TIG	150	8	100
17	A-TIG	150	10	70
18	A-TIG	150	12	85

In the present study L_{18} orthogonal array has been used as shown in Table 5. The outer array is assigned to noise factor and B,C,D are of control factors.

Fig. 5 shows the L18 orthogonal array with factors and their levels.

3.5 Testing of Weldments

3.5.1 Tensile Testing

Tensile test specimens were sampled out from each welded plate as shown schematically in the Fig.1 Dimensions of the sample were according to ASTM E08 standards[18]. Test were performed on "BIS nano servo hydraulic UTM" machine. Maximum load that machine can apply on the specimen is of 25KN. As the specimen is stainless steel and it is ductile in nature the fracture observed is cup and cone type.

Fig. 1: Welded Specimens

Fig. 2: Tensile Test Specimen

3.5.2 Charpy Impact Testing

Charpy impact test specimens were sampled out from each welded plate as shown schematically in the Fig. 3. Dimensions of the sample were according to ASTM E23 standards[21]. Standard specimen size for impact testing is 55 x 10 x 10mm, but thickness of plate used in present study is of 6mm. A nonstandard criterion was employed in order to compare the degree of parts welded trough [19]. V-notch is provided on the specimen as shown in the Fig. with the notch angle of 45º to a depth of 2 mm. Test was conducted on "pendulum impact tester" 300 joules at metallurgy lab.

Fig. 3. Impact Test Specimen

4. RESULT AND DISCUSSION

4.1 Effect of Activated Flux on Tensile and Impact Strength

The comparative analysis of ultimate tensile strength, percentage elongation an impact strength with or without using TiO_2 activated flux is performed each tests was performed one time and the result were analysed. Sum of squares and S/N ratio was calculated for each factor separately in order to determine the effect of different factors on the result. The purpose is to increase the tensile and impact strength of the weldments. The present study shows that the TiO_2 flux has given the high value tensile strength of 655.709 MPa along with percentage elongation (ductility) of 34.404 and impact strength of 167 J. This is very high in comparison to the values of strength (568.056) and ductility (24.985) and impact strength of 132 J without using flux for stainless steel 316.

Table 6 Analysis of Variance for S/N ratios for Tensile Strength

Parameters	DOF	Sum of Square	Mean Squares	F-Value	P-Value
Type of Welding	1	0.70687	0.70687	8.72	**0.018**
Welding Current (A)	2	1.35723	0.67862	8.37	**0.011**
SGFR(l/min)	2	0.88142	0.44071	5.43	**0.032**
Welding Speed(mm/min)	2	0.04867	0.04867	0.30	0.749
Welding type*Current	2	0.32430	0.32430	2.00	0.198
Residual Error	8	0.64844	0.64884		
Total	17	3.96733	3.96733		

In order to determine the parameters which significantly affect the strength of weld metal, investigation of the welding parameters was done using ANOVA analysis. The ANOVA analysis is another powerful tool of Taguchi process which is done after S/N ratio analysis. Error variance and relative importance of the factors are determined in this analysis The S/N ratio was selected based on the larger-the better criterion in order to achieve the optimal parameters. The analysis is made with the help of a software package MINITAB 17.

The ANOVA table obtained from Minitab software is shown in Table 6. It can be stated that type of welding, welding current and SGFR have significant effect on the Tensile strength of the weld zone.

It can be seen clearly that the tensile strength varies linearly with variation in welding type. The Tensile strength is affected most by the variation in welding current to lowest value (i.e. level 1). The main effect plot for S/N ratios between tensile strength and welding current shows that the tensile strength value decreases linearly from low value to the intermediate value and again it increases from intermediate value to high value of current.

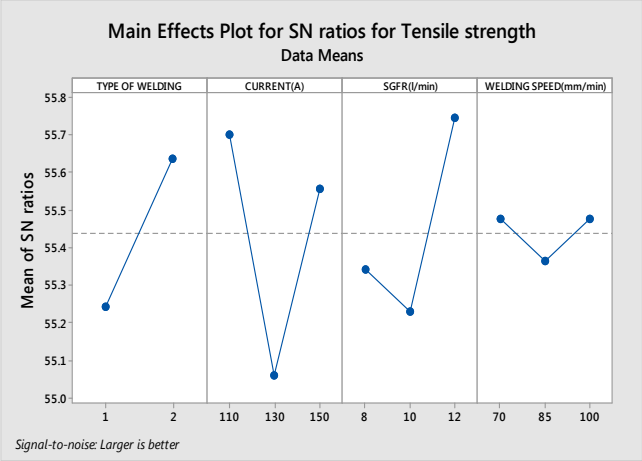

Fig. 4: Main Effect Plot for S/N ratios for Tensile Strength

The main effect of shielded gas flow rate and tensile strength shows that peak stress decreases slightly when gas flow rate decreases from low to intermediate value and increases to the high value. Main effect plot between welding speed and tensile strength indicate that tensile strength in maximum at low and the high value of welding speed and minimum at intermediate value. Now from this we can conclude that welding current (A) has most significant effect on the tensile strength (MPa).From Table 7, it can be stated that type of welding, welding current and SGFR have significant effect on the % Elongation of the weld zone.

Table 7: Analysis of Variance for S/N Ratios for % Elongation

Parameters	DOF	Sum of Square	Mean Squares	F-Value	P-Value
Type of Welding	1	10.6807	10.6807	16.49	**0.004**
Welding Current (A)	2	4.6787	2.3394	3.61	**0.076**
SGFR(l/min)	2	6.6878	3.3439	5.16	**0.036**
Welding Speed(mm/min)	2	1.5002	0.7501	1.16	0.362
Welding type*Current	2	0.5655	0.2827	0.44	0.661
Residual Error	8	5.1824	0.6478		
Total	17	29.295			

Fig. 5 show the signal to noise ratio with welding current, gas flow rate and welding speed response to % elongation. From fig. 5 it can be seen clearly that the % elongation varies linearly with variation in welding type. The impact strength is affected most by the variation in welding current to lowest value (i.e. level 1). The plot for S/N ratios between % Elongation and welding current shows that the %Elongation value decreases linearly from low value to the intermediate value and again it increases from intermediate value to high value of current. The main effect of shielded gas flow rate and % elongation shows that % elongation decreases slightly when gas flow rate increases from low to the high value. Main effect plot between welding speed and % elongation indicate that impact strength in maximum at low and the high value of welding speed and minimum at intermediate value. Now from this we can conclude that

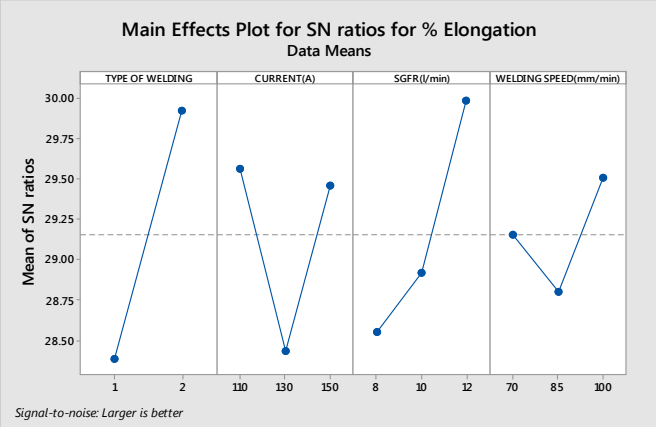

Fig. 5: Main Effect Plot for S/N Ratios for % Elongation

Welding current (A) has most significant effect on the % Elongation.

Table 8: Analysis of Variance for S/N Ratios for Impact Strength

Parameters	DOF	Sum of Square	Mean Squares	F-Value	P-Value
Type of Welding	1	2.1598	2.15976	8.01	**0.022**
Welding Current (A)	2	2.4864	1.24320	4.61	**0.047**
SGFR(l/min)	2	2.4769	1.23843	4.59	**0.047**
Welding Speed(mm/min)	2	0.0478	0.02392	0.09	0.916
Welding type*Current	2	0.7709	0.38544	1.43	0.295
Residual Error	8	2.1566	0.26957		
Total	17	10.0983			

Fig. 6 show the signal to noise ratio with welding current, gas flow rate and welding speed response to impact strength. From the fig.6 it can be seen clearly that the impact strength varies linearly with variation in welding type. The impact strength is affected most by the variation in welding current to lowest value (i.e. level 1).

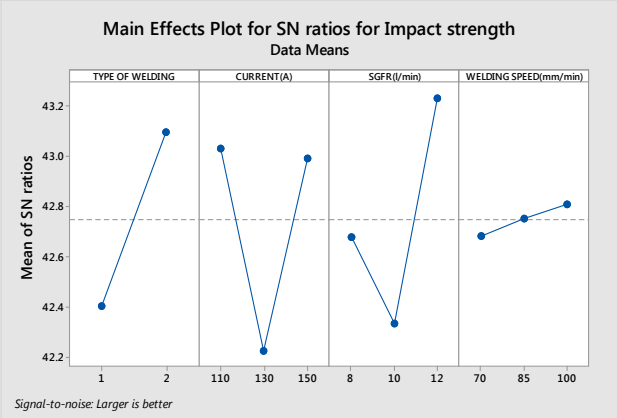

Fig. 6: Main effect plot for S/N ratio for Impact Strength

The main effect plot for S/N ratios between impact strength and welding current shows that the impact strength value decreases linearly from low value to the intermediate value and again it increases from intermediate value to high value of current. The main effect of shielded gas flow rate and peak stress shows that impact strength decreases slightly when gas flow rate decreases from low to intermediate value and increases to the high value. Main effect plot between welding speed and impact strength indicate that impact strength in maximum at low and the high value of welding speed and minimum at intermediate value. Now from this we can conclude that welding current (A) has most significant effect on the impact strength (J).

4.2 Effect of Activated Flux on Microstructure

Fig. 7 shows the microstructure of the weld, HAZ as well as interface of conventional TIG(C-TIG)welding. Primary ferritic mode of solidification occurred in C-TIG welding. During solidification, dendrites of δ-ferrite are formed.

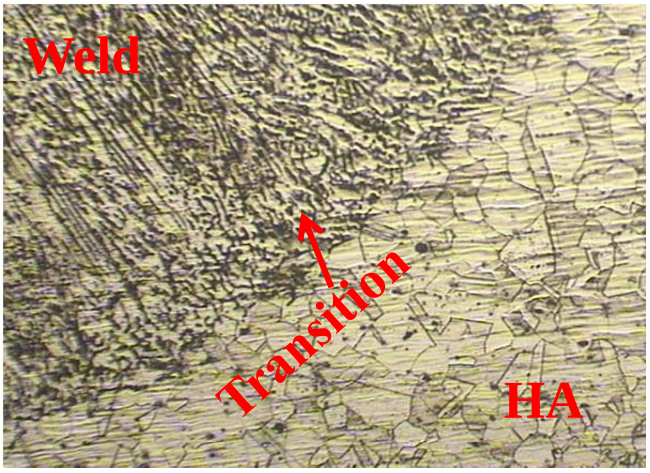

Fig. 7: Microstructure of Weld Bead without Flux TIG Welding

When cooling takes place, δ-ferrite releases their carbon because at low temperature δ-ferrite has less carbon content and converts into austenite. Weld bead consists of equiaxed grain structure with δ-ferrite. Distribution and orientation of equiaxed grain along with δ-ferrite with respect to welding direction were found. The HAZ of conventional TIG welding has coarse grains as compared to base metal.

Fig. 8 shows the microstructure of weld bead of activated TIG (A-TIG) welding with TiO_2 flux. Microstructure shows that much fine dendrites of δ- ferrites were obtained which are small in size (dense) and large amount of austenite were equally distributed continuously throughout the weld bead. Many coarse grains are found in the heat affected zone (HAZ) as compared to C-TIG welding.

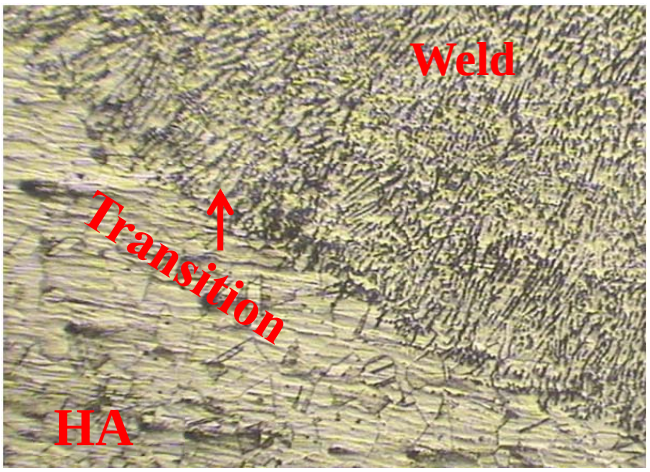

Fig. 8: Microstructure of Weld Bead with TiO_2 Flux TIG Welding

5. CONCLUSIONS

The present work studied the effect of welding process parameters on tensile strength of weldment AISI 316 stainless steel sheet produced by Activated flux tungsten inert gas (A-TIG) welding process. The following conclusions are drawn:

1. The tensile and impact strength is improved to high value by A-TIG. due to TiO_2 flux used. Sample 9 which is of A-TIG shows 15.4 % and 26.51% improvement in tensile and impact strength respectively when compared to sample 1 which is of C-TIG with same parameters.
2. The optimum values of process parameters for weld specimens are 100 mm/min travel speed, 200 A welding current and 12 lit/min gas flow rate.
3. Microstructure shows that specimen with TiO_2 flux have fine grains compare to that without flux, with better depth of penetration.

REFERENCES

[1] Ahmadi, E. and Ebrahimi, A.R., 2012. The effect of activating fluxes on 316L stainless steel weld joint characteristic in TIG welding using the Taguchi method. *Journal of Advanced Materials and Processing*, *1*(1), pp.55-62.

[2] Loureiro, A.R., Costa, B.F.O., Batista, A.C. and Rodrigues, A., 2013. Effect of activating flux and shielding gas on microstructure of TIG welds in austenitic stainless steel. *Science and Technology of Welding & Joining*. pp.315-320

[3] Chern, T.S., Tseng, K.H. and Tsai, H.L., 2011. Study of the characteristics of duplex stainless steel activated tungsten inert gas welds. *Materials & Design*, *32*(1), pp.255

[4] Tseng, K.H. and Hsu, C.Y., 2011. Performance of activated TIG process in austenitic stainless steel welds. *Journal of Materials Processing Technology*,*211*(3), pp.503-512.

[5] Tseng, K.H. and Chuang, K.J., 2012. Application of iron-based powders in tungsten inert gas welding for 17Cr–10Ni–2Mo alloys. *Powder Technology*,*228*, pp.36-46.

[6] Tseng, K.H., 2013. Development and application of oxide-based flux powder for tungsten inert gas welding of austenitic stainless steels. *Powder Technology*, *233*, pp.72-79.

[7] Sándor, T., Mekler, C., Dobránszky, J. and Kaptay, G., 2013. An improved theoretical model for A-TIG welding based on surface phase transition and reversed Marangoni flow. *Metallurgical and Materials Transactions A*, *44*(1), pp.351-361.

[8] Tseng, K.H. and Wang, N.S., 2014. GTA welding assisted by mixed ionic compounds of stainless steel. *Powder Technology*, *251*, pp.52-60.

[9] Tseng, K.H. and Hsu, C.Y., 2011. Performance of activated TIG process in austenitic stainless steel welds. *Journal of Materials Processing Technology*,*211*(3), pp.503-512.

[10] https://uwelding.wordpress.com/

[11] http://www.mydiscounttools.com/estore/articles/welding/weldingequipment.html

[12] Korra, N.N., Vasudevan, M. and Balasubramanian, K.R., 2015. Multi-objective optimization of activated tungsten inert gas welding of duplex stainless steel using response surface methodology. *The International Journal of Advanced Manufacturing Technology*, *77*(1-4), pp.67-81

[13] Karunakaran, N., 2012. Effect of pulsed current on temperature distribution, weld bead profiles and characteristics of GTA welded stainless steel joints.*International Journal of Engineering &Technology*, *2*, pp.1908-1916.

[14] Pamnani, R., Vasudevan, M., Vasantharaja, P. and Jayakumar, T., 2015. Optimization of A-GTAW welding parameters for naval steel (DMR 249 A) by design of experiments approach. *Proceedings of the Institution of Mechanical Engineers, Part L: Journal of Materials Design and Applications*, p.1464420715596455.

[15] Montgomery, D.C., 2008. *Design and analysis of experiments*. John Wiley & Sons

[16] Taguchi, G., 1986. Introduction to quality engineering: designing quality into products and processes.

[17] http://www.azonano.com/article.aspx?ArticleID= 3357.

[18] ASTM E8 Standard Test Methods for Tension Testing of Metallic Materials. Annualbook of ASTM standards, ASTM International.

[19] ASTM E23 Standard Test Methods for Notched Bar Impact Testing of Metallic Materials. Annual book of ASTM standards, ASTM International.

[20] Sakthivel, P. and Sivakumar, P., 2014. Effect of Vibration in Tig And Arc Welding Using AISI 316 Stainless Steel. *International Journal of Engineering, Research and Science & Technology*, *3*(4), pp.116-130.